doi: 10.34248/bsengineering.1703012



Research Article

Volume 8 - Issue 5: 1406-1414 / September 2025

CHAOTIC SPEED CONTROL OF A DC MOTOR USING THE SPROTT-A SYSTEM FOR ROBOTIC END-EFFECTOR APPLICATIONS

Yusuf HAMİDA EL NASER^{1*}, Berk DEMİRSOY², Kenan ERİN³, Mert Süleyman DEMİRSOY¹

¹Sakarya University of Applied Sciences, Faculty of Tecnology, Department of Mechatronic Engineering, 54050, Sakarya, Türkiye ²Kormas Electric Motor inc., TOSB OSB, 41420, Kocaeli, Türkiye

³Tarsus University, Faculty of Engineering, Department of Mechanical Engineering, 33400, Mersin, Türkiye

Abstract: This study investigates the use of chaotic speed control, based on the Sprott-A chaotic system, for improving the performance and stability of DC motor-driven robotic end-effector mixers. The chaotic differential equations were implemented and numerically solved in MATLAB/Simulink using the fourth-order Runge–Kutta method, and the resulting time series were analyzed. Among the variables generated, the X_t signal was selected for pulse-width modulation (PWM) due to its smooth dynamic characteristics. This signal was scaled to match the 0–100% duty cycle range and applied to the motor driver as a control input. The chaotic control system was realized both through analog circuit simulation in OrCAD and experimentally using an STM32F407 microcontroller. Time series, phase portraits, and oscilloscope outputs confirmed the consistency between simulation and hardware implementations. Compared to chaotic Y_t and Z_t signals, the chaotic X_t based PWM control reduced motor vibrations and provided more stable speed regulation. These results demonstrate the feasibility and effectiveness of chaotic dynamics for real-time motor control in robotic mixing applications, offering a robust alternative to traditional deterministic methods.

Keywords: Robotics, Chaos theory, Motor speed control, PWM

*Corresponding author: Sakarya University of Applied Sciences, Faculty of Tecnology, Department of Mechatronic Engineering, 54050, Sakarya, Türkiye E mail: yusufelnaser@subu.edu.tr (Yusuf HAMİDA EL NASER)

E mail: yusufelnaser@subu.edu.tr (Yusuf HAMIDA EL NASER)
Yusuf HAMIDA EL NASER https://orcid.org/0000-0003-4757-6288

Berk DEMİRSOY
Kenan ERİN

Mert Sülevman DEMİRSOY

https://orcid.org/0009-0003-3489-7346 https://orcid.org/0000-0003-4714-1161 https://orcid.org/0000-0002-7905-2254 Received: May 20, 2025 Accepted: July 23, 2025 Published: September 15, 2025

Cite as: Hamida El Naser Y, Demirsoy B, Erin K, Demirsoy MK. 2025. Chaotic speed control of a dc motor using the sprott-a system for robotic end-effector applications. BSJ Eng Sci, 8(5): 1406-1414.

1. Introduction

The precise regulation of mixer speed in robotic and industrial applications remains a cornerstone of process efficiency, particularly in fields such as food engineering, pharmaceuticals, and advanced materials. As the demand for uniformity, adaptability, and energy efficiency intensifies, control methodologies have evolved from deterministic frameworks to encompass nonlinear and chaotic dynamics, particularly within robotic systems.

Variable-speed mixers have demonstrated superior performance across diverse mixing scenarios. Simanjorang et al. showed that maintaining consistent stirring speeds enables uniform viscosity during nanoparticle dispersion (Simanjorang et al., 2022) Brushless DC (BLDC) motors further enhance this stability with high efficiency and reduced energy losses, as observed by Nayak and Shivarudraswamy (Nayak and Shivarudraswamy, 2020). Feedback-enhanced control architectures are increasingly employed to improve realtime mixer response. Shih et al. introduced a vision-based feedback system capable of adjusting DC motor speed based on material visual cues (Shih et al., 2017).

Recent advances in Cartesian robotic systems have highlighted the growing importance of integrating intelligent control strategies, particularly in applications dynamic environments and involving manipulation tasks. Among the most widely applied techniques, impedance and admittance frameworks have proven effective for achieving compliant motion and safe physical interactions. Mayr and Salt-Ducaju introduced a Cartesian impedance controller that stabilizes motion under contact-rich conditions, while Yang et al. demonstrated the benefits of admittance control in dual-arm robots for facilitating human-robot interaction (Yang et al., 2019; Mayr and Salt-Ducaju, 2022). Complementing these approaches, Portillo-Vélez et developed an optimization-based impedance regulation method to maintain operational safety within force boundaries (Portillo-Vélez et al., 2015). To manage uncertainties and dynamic variability, adaptive control methodologies have gained prominence. Al Khudir and De Luca focused on acceleration level control by exploiting kinematic redundancy, and Kazemipour et al. addressed time-varying constraints through real-time adaptive



kinematic adjustments (Al Khudir and De Luca, 2018; Kazemipour et al., 2022). Fuzzy logic-based control has further expanded the adaptability of robotic systems, as seen in the work of Li et al. and Chen et al., who demonstrated fuzzy controller designs that enhance trajectory tracking and resilience against environmental disturbances (Li et al., 2017 and Chen et al., 2022). In the domain of robotic manipulators, ILC has been successfully integrated with servo motors to enhance tracking accuracy in cyclic operations, such as robotic welding, pick-and-place tasks, and repetitive force control. Studies have shown that combining ILC with conventional Proportional-Integral-Derivative (PID) or model-based controllers leads to faster convergence and robustness against model uncertainties. For instance, adaptive ILC schemes have been proposed to address parameter variations and nonlinearities in actuator dynamics, enabling consistent performance even under fluctuating load conditions (Demirsoy et al. 2024). This capability becomes especially valuable in visual servoing tasks, where image-based feedback is incorporated to adjust the robot's end-effector trajectory in real time (El Naser et al., 2024). In such cases, the synergy between ILC and computer vision algorithms allows for the compensation of visual disturbances, delays, or occlusions, leading to improved spatial accuracy and adaptive behavior in unstructured environments.

Addressing high-dimensional and redundant systems, Flacco et al. proposed strategies for managing hard joint constraints without compromising task execution (Flacco et al., 2015). Liu et al. advanced motion generation using dynamic movement primitives (DMPs) with embedded feedback to achieve adaptive and human-like motions (Liu et al., 2020). A growing body of research explores chaos theory as a powerful framework for robotic control. Miranda-Colorado et al. introduced chaotic modulation in joint manipulators, revealing improved maneuverability through nonlinear trajectories (Miranda-Colorado et al., 2018). Ren et al. (2015) applied multiple chaotic central pattern generators (CPGs) for legged locomotion, enabling adaptive fault compensation. Zang et systematically reviewed chaos-based robotic applications, highlighting its potential for navigation, exploration, and unpredictable motion planning (Zang et al., 2016). Chaos stabilization techniques such as the OGY method and Hamiltonian energy feedback further illustrate how nonlinear control enhances system robustness (Huang et al., 2016; Ahrabi and Kobravi, 2019). Li et al. proposed Lorenz-based bounded coverage strategies for mobile robots, affirming the utility of chaos in task diversification (Li et al., 2016). In parallel, the control of robotic end-effectors in mixing applications has evolved to incorporate novel actuator technologies and sensor-driven feedback systems. Tanaka et al. designed pneumatic suction-based end-effectors for depalletizing tasks, and Telegenov et al. introduced an underactuated gripper with breakaway clutch mechanisms for adaptive manipulation (Telegenov et al., 2015; Tanaka et al., 2020). Xiang et al. integrated soft robotics into end-effector design, enabling delicate and responsive material handling (Xiang et al., 2019). Zhao et al. implemented vision-based trajectory compensation to enhance flexibility in manufacturing robots, while Khan et al. proposed a virtual force-tracking impedance control scheme for precise trajectory tracking in mixing contexts (Zhao et al., 2024; Khan et al., 2025). These studies outline a multidimensional research landscape where impedance control, adaptive strategies, fuzzy logic, and chaosinformed models converge to address the challenges of dynamic robotic manipulation. The integration of chaotic dynamics into speed control and motion generation represents a promising direction for future robotic mixers, especially in environments demanding flexibility, responsiveness, and control robustness.

Recent experimental work demonstrated the integration of chaotic speed control with robotic mixing systems, where chaotic signals derived from the Halvorsen, Newton-Leipnik, Hadley, and Sprott A attractors were used to modulate the DC motor speed of a Cartesian robot's end-effector mixer (Yagmur and Kutlu, 2024). Furthermore, the application of chaotic speed modulation has also been extended to bioreactor systems, where a hybrid shaft mixer controlled by chaotic algorithms (Hadley, Halvorsen, Lorenz, and Sprott-A) significantly enhanced methane production and combustion quality compared to conventional fixed-speed methods (Sarıkaya et al., 2025). These findings confirm the practical relevance of chaos-based speed modulation in robotic mixing applications and support its further investigation within Cartesian robotic frameworks.

Despite the extensive body of research on mixer speed control using classical techniques such as PID controllers, fuzzy logic, and sliding mode control, significant limitations persist, particularly in environments characterized by nonlinearity, variable material properties, and dynamic operational constraints. Existing studies primarily focus on deterministic control methods that assume relatively stable mixing conditions and do not adequately address the performance fluctuations observed in complex, time-varying mixing tasks. Furthermore, while the application of chaotic dynamics to motor control has been explored at a theoretical level (particularly in the context of chaotization and stability control of standalone DC motors) the integration of chaos theory into robotic end-effector systems performing mixing tasks remains largely unexplored.

This study aims to address these gaps by proposing a novel approach in which a DC motor, mounted as an endeffector on a Cartesian robotic system, performs the mixing operation with its speed dynamically modulated based on scaled outputs from the Sprott-A chaotic differential equations. Unlike traditional speed profiles, the use of chaotic signals introduces non-repetitive, yet bounded variations in motor speed, thereby enhancing turbulence and improving fluid mixing efficiency. This method bridges the domains of nonlinear dynamics,

robotic control, and process engineering by embedding chaos-derived trajectories into the actuator control loop. Through simulation-based validation, the proposed system is expected to enhance mixing performance in terms of homogeneity and process speed, particularly in scenarios involving high-viscosity or heterogeneous mixtures. The study contributes a novel intersection between chaos theory and robotic mixing applications, filling a critical gap in the literature and offering a foundation for future experimental and industrial deployment.

2. Materials and Methods

In this study, the speed control of the DC motor integrated into the robotic end-effector was performed by chaotically modulating the PWM (Pulse Width Modulation) signal based on the *z*-component of the "A" system presented by J. C. Sprott in his 1994 paper titled "Some Simple Chaotic Flows" (Sprott, 1994). The corresponding differential equation system is provided in equation 1, with initial conditions defined as x(0)=0, y(0)=1 and z(0)=0.

$$\dot{x} = y
\dot{y} = yz - x
\dot{z} = 1 - y^2$$
(1)

2.1. Dynamic analysis and stability assessment of the system

When analyzing the behavior of the system in the vicinity of the point (0,0,0), the differential equations constituting the system are set equal to zero, as shown in equation 2, in order to identify possible equilibrium points. However, upon attempting to solve the system of equations simultaneously, it becomes evident that no valid solution exists near this point. Consequently, the system does not exhibit a critical (equilibrium) point at (0,0,0).

$$\dot{x} = y = 0, \dot{y} = yz - x = 0, \dot{z} = 1 - y^2 = 0$$
 (2)

The Jacobian matrix of the system, as presented in equation 3, is analyzed to investigate the local stability characteristics of the system around potential equilibrium points.

$$J = \begin{bmatrix} 0 & 1 & 0 \\ -1 & z & y \\ 0 & -2y & 0 \end{bmatrix}$$
 (3)

To examine the conservativeness of the system, the elements along the main diagonal of the Jacobian matrix are summed, as shown in equation 4, which represents the volumetric divergence of the system. However, due to the absence of an identifiable equilibrium point, conservativeness cannot be conclusively determined through this method alone.

$$\nabla \cdot \vec{F} = \frac{\partial \dot{x}}{\partial x} + \frac{\partial \dot{y}}{\partial y} + \frac{\partial \dot{z}}{\partial z} = 0 + z + 0 = z \tag{4}$$

Therefore, further analysis such as evaluating the Kaplan-

Yorke dimension is necessary to draw a definitive conclusion (Sarıkaya et al., 2024). Owing to these distinctive characteristics, the Sprott-A chaotic system is considered a special case and has been selected for use in this study.

The MATLAB/Simulink model of the Sprott-A chaotic system is presented in Figure 1.

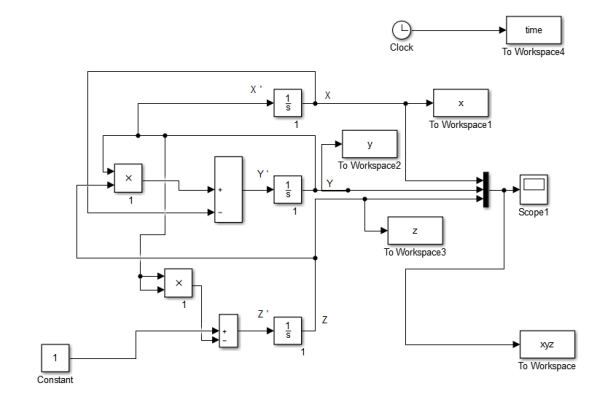


Figure 1. Modeling of the sprott-a chaotic system using simulink.

The Lyapunov exponents of the system are calculated using the formula given in equation 5.

$$\lambda_{Y} = \lim_{n \to \infty} \frac{1}{n} \sum_{k=0}^{n-1} \ln \left| \frac{x_{k} - y_{k}}{x_{0} - y_{0}} \right|$$
 (5)

The Lyapunov exponent graph, plotted based on the expression in Equation 5, is shown in Figure 2.

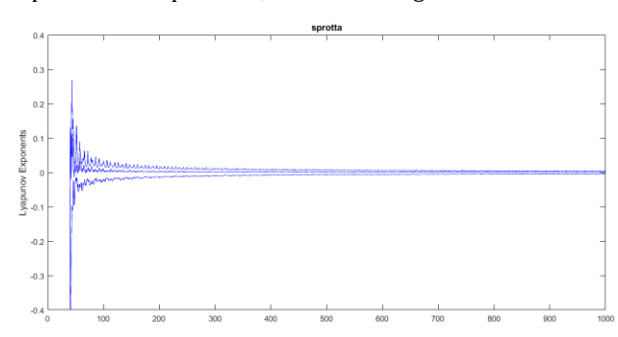


Figure 2. Determination of the system's Lyapunov exponents.

According to the results, the Lyapunov exponents are approximately calculated as λ_1 =0.004, λ_2 =0 and λ_3 =-0.004. Based on these values, the Kaplan-Yorke (Lyapunov) dimension is computed as in equation 6.

$$\lambda_{KY} = j + \frac{\lambda_1 + \lambda_2}{|\lambda_3|} = 2 - \frac{0.004}{|-0.004|} = 3$$
 (6)

In three-dimensional chaotic systems, the Kaplan–Yorke dimension typically lies between 2 and 3. However, obtaining an exact value of 3 indicates that the system is conservative, meaning it does not exhibit volumetric contraction over time. Instead, the system tends to fill the entire three-dimensional phase space as time approaches infinity. Furthermore, based on this interpretation, the equality expressed in equation 7 can also be derived.

$$\frac{1}{V}\frac{dV}{dt} = \frac{\partial \dot{x}}{\partial x} + \frac{\partial \dot{y}}{\partial y} + \frac{\partial \dot{z}}{\partial z} = \lambda_1 + \lambda_2 + \lambda_3 = 0 \tag{7}$$

Variations in the parameters of a nonlinear system of differential equations can directly influence the system's dynamic behavior. Depending on the nature and extent of these changes, the system may exhibit different types of stability characteristics, including point stability, limit cycle behavior, quasi-periodic or quasi-chaotic responses, fully developed chaos, or even instability. The influence of parameter variations (particularly on the system's transition to chaos) can be effectively analyzed using bifurcation diagrams, which provide a visual representation of how the system's qualitative behavior changes with respect to key parameter values.

The bifurcation diagram shown in Figure 3 illustrates the variation in the system's chaotic behavior with respect to changes in the coefficient of the y parameter in Equation 1 ($\dot{x} = y$), as it varies within the range [0,3].

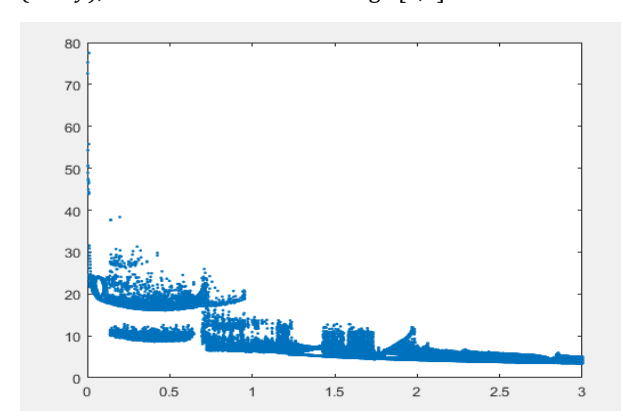


Figure 3. Effect of varying the coefficient of the y parameter in Equation 1 within the range [0,3] on the system's behavior.

The bifurcation diagram presented in Figure 4 illustrates in Figure 4 how the system's chaotic behavior varies with changes in the constant term added to the $-y^2$ expression in Equation 1 ($\dot{z}=1-y^2$), as this constant is varied within the range [0,3].

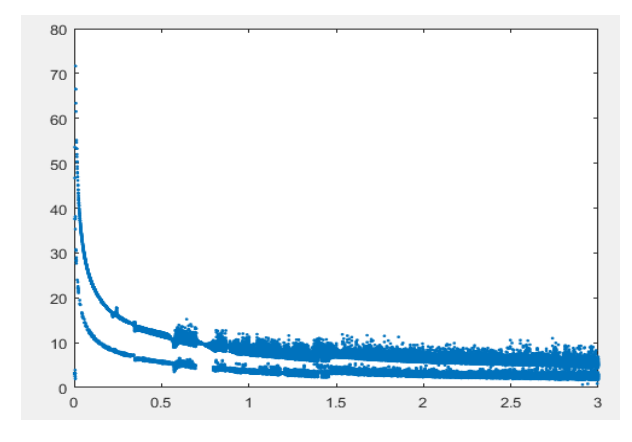


Figure 4. Effect of varying the constant added to the $-y^2$ term in Equation 1 within the range [0,3] on the system's behavior.

3. Results and Discussion

This section presents the analog implementation of the chaotic system to verify its dynamic characteristics in a physical environment.

In order to validate the numerical behavior of the system under real conditions, an analog circuit implementation was carried out. This implementation enables the observation of the system's dynamic response through physical measurements. Time series, phase portraits, and oscilloscope outputs were obtained to analyze the temporal and state-space behavior of the chaotic system. These experimental signals not only verify the theoretical simulations but also provide insight into the circuit-level realizability of the chaotic dynamics. The use of an oscilloscope facilitates real-time monitoring of the system's variables, allowing for a visual comparison of analog trajectories with simulated results. The results obtained in this section serve as an essential step toward confirming the physical feasibility and consistency of the Sprott-A chaotic system. The system's analog realizations in the simulation environment are presented in Figure 5, (hardware-based) while the experimental implementation is shown in Figure 6.

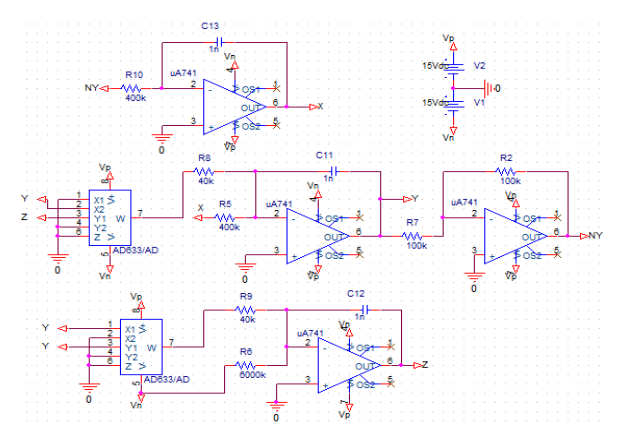


Figure 5. Analog simulation of the system in OrCAD.

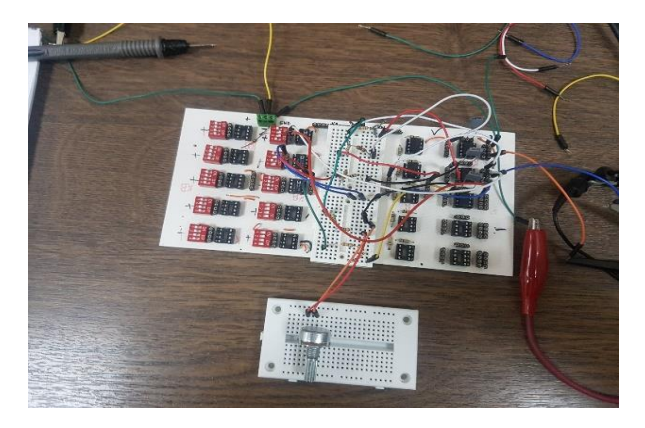


Figure 6. Experimental observation of the system's analog implementation.

The time series outputs obtained from the PSpice software are presented in Figure 7, while the corresponding results from the MATLAB software are shown in Figure 8.

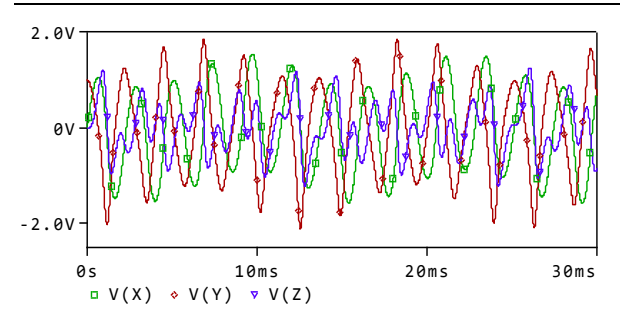


Figure 7. Time series outputs of the system obtained from PSpice software

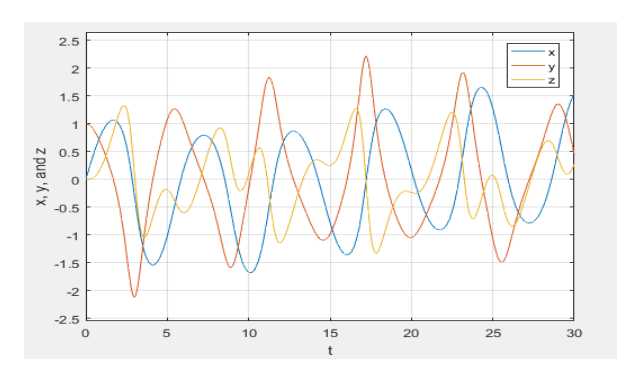


Figure 8. Time series outputs of the system obtained from MATLAB software.

The DAC channels of the STM32F407 microcontroller were configured to output the computed x, y and z signals in real time. These outputs were connected to an oscilloscope, enabling direct observation of the phase relationships between the chaotic variables. Additionally, the z signal was scaled and mapped to generate a PWM signal through one of the timer modules on the microcontroller. This PWM output was then used to control the speed of a DC motor connected to the robotic end-effector.

The two-dimensional phase portraits are presented in Figure 9, and the oscilloscope outputs are shown in Figure 10.

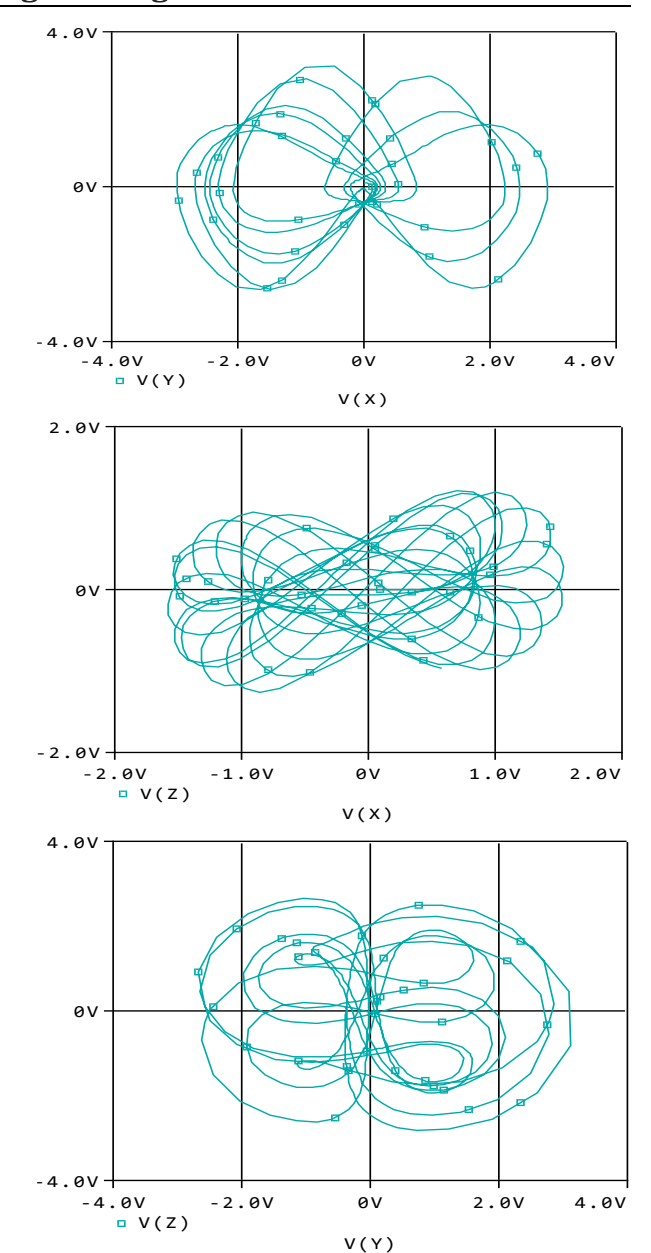


Figure 9. Phase portraits of the system obtained from PSpice outputs.

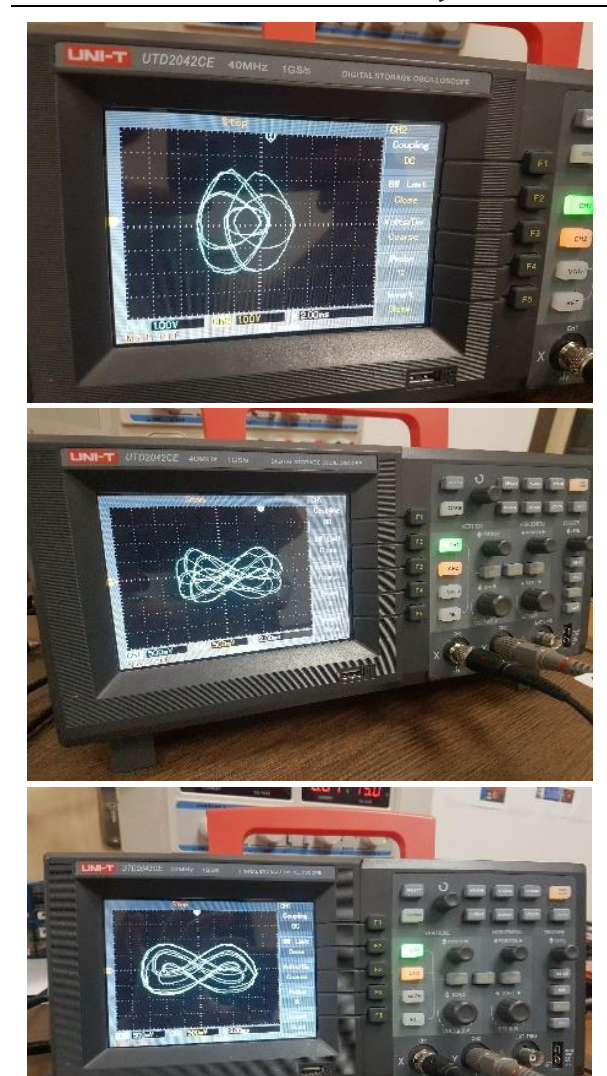


Figure 10. Oscilloscope images of the system's phase portraits.

The microcontroller-based hardware implementation of the Sprott-A chaotic system was used to control the speed of the DC motor mounted on the robotic end-effector. The system of differential equations defining the Sprott-A attractor was solved in the MATLAB environment, and the resulting time series data for the variables x, y and z were transferred to the microcontroller. For this implementation, the STM32F407 Discovery board, based on a 32-bit ARM Cortex-M4 processor, was used as shown in Figure 11. This microcontroller was selected due to its high processing speed and ease of integration with MATLAB/Simulink, enabling code generation and deployment without the need for manual programming.



Figure 11. STM32F407 Discovery development board.

In this study, the Sprott-A chaotic differential equation system was first implemented in the MATLAB/Simulink software. The Runge-Kutta 4th-order (RK4) algorithm was employed to numerically solve the system. After solving the equations, the resulting chaotic signals were used to generate phase diagrams (specifically X-Y, Y-Z, and X-Z plots) which were visualized on an oscilloscope using the DAC outputs of the microcontroller. Among the generated time series signals (X, Y, and Z), the Z signal was further utilized as a PWM input to control the speed of a DC motor. The MATLAB/Simulink block diagram used for programming the microcontroller is shown in Figure 12.

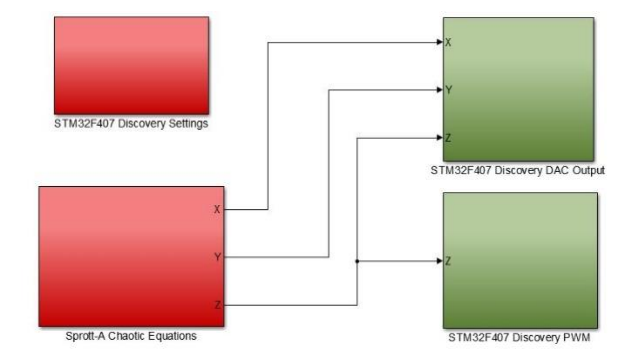


Figure 12. MATLAB/Simulink block diagram for the STM32F407 Discovery board.

The time series of the Sprott-A chaotic system analyzed in the MATLAB software are shown, upon examination of these time series, it was observed that the X_t signal exhibits smoother rising and falling transitions compared to the Y_t and Z_t signals. For this reason, the X_t signal was selected as the basis for generating the PWM (Pulse Width Modulation) signal used in motor speed control. When the Y_t and Z_t signals were applied as PWM inputs, the rapid fluctuations in their amplitude caused the motor to exhibit excessive vibration due to frequent and abrupt changes in speed.

A closer analysis of the X_t signal revealed that its amplitude ranges approximately between 4.3 and -3.9. However, this range is not directly suitable for PWM-based motor control, where the duty cycle typically needs to vary within a 0–100% interval. Therefore, the X_t signal was first scaled mathematically to fit within this interval. The scaling formula used for this purpose is provided in equation 8.

$$PWM = (X + 3.9) * 12 (8)$$

According to this transformation, the resulting PWM duty cycle varies between 0% and approximately 98.4% depending on the instantaneous value of X_t . This mapping enables smoother motor operation with significantly reduced vibration compared to the use of the other chaotic signals.

After the mathematical operations of the chaotic system were performed in MATLAB/Simulink, the system was implemented and controlled on a microcontroller. The resulting PWM signal was used to drive a DC motor equipped with an encoder. The experimental setup is shown in Figure 13. In this setup, the L298N motor driver was used to interface the microcontroller with the motor.

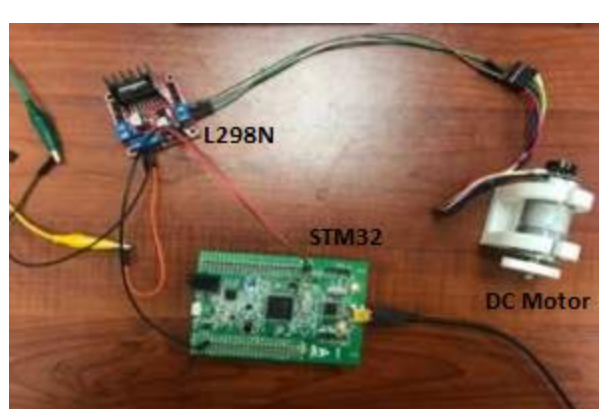


Figure 13. The experimental setup.

The motor speed was controlled chaotically by converting the X_t time series into a PWM signal. The duty cycle of the generated PWM signal was examined using an oscilloscope, and the corresponding waveform is presented in Figure 14.

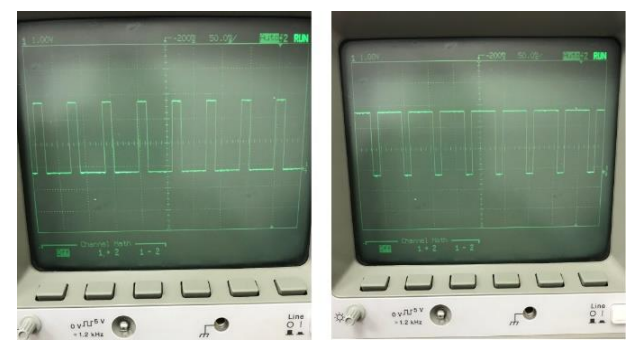


Figure 14. The generated PWM signal.

The findings of this study confirm the practical benefits of implementing chaos-based speed control in robotic mixing systems. By using the X_t component of the Sprott-A chaotic system (scaled appropriately to generate a PWM signal) the motor speed was modulated in a non-repetitive yet bounded manner. This led to significantly smoother motor behavior with reduced mechanical vibration, especially when compared to PWM signals derived from the Y_t and Z_t time series. The superior performance of the X_t driven control signal is attributed to its gradual transitions and lower frequency oscillations, which reduce abrupt torque fluctuations and thus contribute to mechanical stability.

The findings of this study provide compelling evidence supporting the practical benefits of chaotic speed modulation in robotic mixer applications. By employing the X_t signal from the Sprott-A chaotic attractor as a basis for PWM signal generation, a more stable and vibrationfree control of the DC motor was achieved, particularly in comparison to PWM signals derived from Y_t and Z_t signals. This outcome is consistent with previous studies suggesting that non-repetitive, smooth input signals can enhance actuator performance by minimizing torque fluctuations and mechanical resonance (Miranda-Colorado et al., 2018; Khan et al., 2025). Unlike conventional fixed-speed or deterministically controlled mixing systems, the chaotic control paradigm introduces bounded yet dynamically rich variations in motor speed. This facilitates enhanced turbulence and material dispersion, which are known to be critical for achieving homogeneity in high-viscosity or multi-phase mixtures (Simanjorang et al., 2022; Nayak & Shivarudraswamy, 2020). The observed improvements in motor stability and responsiveness are especially significant in the context of robotic end-effectors, where frequent changes in position and load may otherwise destabilize conventional controllers. Moreover, the successful implementation of the Sprott-A system in analog (OrCAD), numerical (MATLAB), and real-time (STM32 microcontroller) environments underscores the feasibility of embedding chaos-based control into physical systems. This multilevel verification aligns with findings in the literature demonstrating the practical realizability of chaotic control models when implemented with appropriate scaling and feedback mechanisms (Zang et al., 2016; Ahrabi & Kobravi, 2019).

The integration of chaos theory into mixer speed control addresses several limitations observed in classical control approaches such as PID or fuzzy logic, which often assume time-invariant system dynamics and linear responses (Li et al., 2017; Chen et al., 2022). While these methods offer satisfactory performance under nominal conditions, they lack the adaptability required for dynamic environments—particularly in mixing scenarios involving fluctuating material properties or non-Newtonian fluids. The chaotic control strategy used in this study overcomes these shortcomings by embedding variability directly into the control signal without compromising boundedness or

stability. Additionally, the analog and oscilloscope-based observations confirm that chaotic signals maintain structural coherence even after hardware conversion and digital-to-analog transformation. This result is particularly relevant for control systems relying on real-time feedback, where signal fidelity is crucial for achieving deterministic outcomes from nonlinear dynamics (Huang et al., 2016; Portillo-Vélez et al., 2015).

The results of this study also resonate with recent experimental investigations into chaos-driven robotic mixing systems (Yagmur & Kutlu, 2024) and chaotic modulation in bioreactor configurations (Sarıkaya et al., 2025), which have shown improved process outcomes such as enhanced biogas yield and reduced energy consumption. These findings collectively support the broader applicability of chaos-informed control strategies across various sectors including biotechnology, materials science, and autonomous robotics. Nevertheless, some limitations remain. The current implementation focused solely on the speed control aspect of the mixing mechanism. Future studies could extend this approach by integrating chaotic trajectory modulation for robotic arms, as proposed in central pattern generator (CPG)based locomotion studies (Ren et al., 2015), or by applying hybrid chaotic controllers that combine force and position control (Mayr & Salt-Ducaju, 2022; Khan et al., 2025). Additionally, a comparative evaluation between different chaotic attractors (e.g., Lorenz, Rössler, Halvorsen) may reveal further insights into system responsiveness and mixing efficiency.

4. Conclusion

This study demonstrated the applicability of the Sprott-A chaotic system in various domains by developing its MATLAB-based numerical model, analog circuit implementation in OrCAD, and microcontroller-based real-time control application. By solving the system's differential equations, time series data corresponding to the variables X_t , Y_t and Z_t were obtained. Among these, the *X_t* signal was selected for generating a PWM control signal due to its smoother dynamic behavior. When applied to a DC motor, the X_t based PWM signal enabled more stable motor speed regulation and significantly reduced mechanical vibration, which is typically observed when using the more abrupt Y_t or Z_t signals. The successful analog and embedded realizations validate the physical feasibility of chaos-based control for robotic mixer applications. Moreover, the findings support the potential of chaotic signals as a superior alternative to traditional deterministic controllers, especially in nonlinear, timesensitive, and high-precision systems. The approach serves as a foundational step for extending chaosinformed control techniques into more complex robotic mixing architectures.

In summary, the study demonstrates that chaotic control can be practically implemented on microcontroller-based systems to improve mixer behavior in robotic endeffectors. The approach not only enhances performance

and energy efficiency but also provides a robust control alternative suitable for nonlinear, high-viscosity, or dynamically changing environments.

In future studies, the design of an industrial mixing system using a delta robot and chaos-based control strategies is planned, with two distinct control approaches to be investigated. The first approach involves transmitting chaotic time series to the servo motors controlling the delta robot's three axes, thereby inducing chaotic variation in the spatial position of the end-effector. This motion is expected to create a dynamically shifting mixing pattern across the workspace. In the second approach, rather than modulating the robot's position, the focus will shift to directly altering the speed of the mixing motor using a chaotic signal. This aims to achieve efficient mixing through speed variability while maintaining a fixed spatial trajectory. Both strategies will be comparatively evaluated to determine their impact on mixing homogeneity, energy efficiency, and control robustness in industrial settings.

Author Contributions

The percentages of authors' contributions are given below. All authors have reviewed and approved the article.

	Y.H.E.N.	B.D.	K.E.	M.S.D.
С	25	30	25	20
D	40	30	10	10
S	10	10	40	40
DCP	25	25	25	25
DAI	25	25	25	25
L	20	30	30	20
W	30	40	15	15
CR	40	40	10	10
SR	10	40	40	10
PM	20	20	40	20
FA	10	30	30	30

C=Concept, D= design, S= supervision, DCP= data collection and/or processing, DAI= data analysis and/or interpretation, L= literature search, W= writing, CR= critical review, SR= submission and revision, PM= project management, FA= funding acquisition.

Conflict of Interest

The authors declare that they have no conflict of interest in this study.

Ethical Approval Statement

Since this study did not involve any studies on animals or humans, ethics committee approval was not obtained.

References

- Ahrabi AR, Kobravi H. 2019. Chaos control in chaotic dynamical systems via auto-tuning Hamilton energy feedback. Turk J Forecast. 3(2): 47-53.
- Al Khudir K, De Luca A. 2018. Faster motion on Cartesian paths exploiting robot redundancy at the acceleration level. IEEE Robot Autom Lett, 3(4): 3553-3560.
- Chen R, Wang C, Wei T, Liu C. 2022. A composable framework for policy design, learning, and transfer toward safe and efficient industrial insertion. In: 2022 October–2022 IEEE/RSJ Int Conf Intell Robots Syst (IROS), Kyoto, Japan, pp: 8894-8901.
- Demirsoy MS, El Naser YH, Sarıkaya MS, Peker NY, Kutlu M. 2024. Development of elbow rehabilitation device with iterative learning control and internet of things. Turk J Eng, 8(2): 370-379.
- El Naser YH, Karayel D, Demirsoy MS, Sarıkaya MS, Peker NY. 2024. Robotic arm trajectory tracking using image processing and kinematic equations. Black Sea J Eng Sci, 7(3): 436-444.
- Flacco F, De Luca A, Khatib O. 2015. Control of redundant robots under hard joint constraints: Saturation in the null space. IEEE Trans Robot, 31(3): 637-654.
- Huang Y, Huang Q, Wang Q. 2016. Chaos and bifurcation control of torque-stiffness-controlled dynamic bipedal walking. IEEE Trans Syst Man Cybern Syst, 47(7): 1229-1240.
- Khan H, Lee MC, Suh J, Kim R. 2025. Enhancing robot end-effector trajectory tracking using virtual force-tracking impedance control. Adv Intell Syst, 7(2): 2400380.
- Kazemipour A, Khatib M, Al Khudir K, Gaz C, De Luca A. 2022. Kinematic control of redundant robots with online handling of variable generalized hard constraints. IEEE Robot Autom Lett, 7(4): 9279-9286.
- Li C, Song Y, Wang F, Wang Z, Li Y. 2016. A bounded strategy of the mobile robot coverage path planning based on Lorenz chaotic system. Int J Adv Robot Syst, 13(3): 107.
- Li S, Xu M, Quo J, Wang B, Hong Y. 2017. Design of fuzzy cross coupling controller for Cartesian robot. In: 2017 Int Conf Appl Math Model Stat Appl (AMMSA), Atlantis Press, pp: 427-431.
- Liu N, Zhou X, Liu Z, Wang H, Cui L. 2020. Learning peg-in-hole assembly using Cartesian DMPs with feedback mechanism. Assembly Autom, 40(6): 895-904.
- Mayr M, Salt-Ducaju JM. 2022. A C++ implementation of a Cartesian impedance controller for robotic manipulators. arXiv preprint arXiv:2212.11215 (accessed date: September 2, 2025).
- Miranda-Colorado R, Aguilar LT, Moreno-Valenzuela J. 2018. A model-based velocity controller for chaotization of flexible joint robot manipulators: Synthesis, analysis, and experimental evaluations. Int J Adv Robot Syst, 15(5): 1729881418802528.

- Nayak DS, Shivarudraswamy R. 2020. Solar fed BLDC motor drive for mixer grinder using a buck-boost converter. Bull Electr Eng Inform, 9(1): 48-56.
- Portillo-Vélez RDJ, Rodriguez-Angeles A, Cruz-Villar CA. 2015. An optimization-based impedance approach for robot force regulation with prescribed force limits. Math Probl Eng, 2015:918301.
- Ren G, Chen W, Dasgupta S, Kolodziejski C, Wörgötter F, Manoonpong P. 2015. Multiple chaotic central pattern generators with learning for legged locomotion and malfunction compensation. Inf Sci, 294:666-682.
- Sarıkaya MS, El Naser YH, Kaçar S, Yazıcı İ, Derdiyok A. 2024. Chaotic-based improved Henry gas solubility optimization algorithm: Application to electric motor control. Symmetry, 16(11): 1435.
- Sarıkaya MS, Demirel O, Kaçar S, Derdiyok A. 2025. Modelling and chaotic based parameter optimization of sliding mode controller. J Math Sci Model, 8(2): 42-54.
- Shih CL, Hsu JH, Chang CJ. 2017. Visual feedback balance control of a robot manipulator and ball-beam system. J Comput Commun, 5(9): 8-18.
- Simanjorang MR, Susanto H, Bukhori ML. 2022. Design and construction of mixer with variable speed for manufacturing nanoparticle composite materials. Teknika STTKD J Tek Electron Eng, 8(2): 257-266.
- Sprott JC. 1994. Some simple chaotic flows. Phys Rev E, 50(2): R647.
- Tanaka J, Ogawa A, Nakamoto H, Sonoura T, Eto H. 2020. Suction pad unit using a bellows pneumatic actuator as a support mechanism for an end effector of depalletizing robots. ROBOMECH J, 7: 1-30.
- Telegenov K, Tlegenov Y, Hussain S, Shintemirov A. 2015. Preliminary design of a three-finger underactuated adaptive end effector with a breakaway clutch mechanism. J Robot Mechatron, 27(5): 496-503.
- Xiang C, Guo J, Rossiter J. 2019. Soft-smart robotic end effectors with sensing, actuation, and gripping capabilities. Smart Mater Struct, 28(5): 055034.
- Yagmur D, Kutlu M. 2024. 3D chaotic mixing application for polymer production. Phys Scr, 99(4): 045210.
- Yang J, Xie Y, Feng M, Li J. 2019. Design and implementation of admittance control for a dual-arm robot under space limitation. In: MATEC Web Conf. 256: 02010.
- Zang X, Iqbal S, Zhu Y, Liu X, Zhao J. 2016. Applications of chaotic dynamics in robotics. Int J Adv Robot Syst, 13(2): 60.
- Zhao N, Murakami K, Yamakawa Y. 2024. Vision-based trajectory dynamic compensation system of industrial robot. Int J Adv Manuf Technol, 131(12): 6013-6026.